

# Combining Mass Spectrometry and NMR Improves Metabolite Detection and Annotation

Fatema Bhinderwala,<sup>†,‡</sup> Nishikant Wase,<sup>‡</sup> Concetta DiRusso,<sup>‡,§</sup> and Robert Powers\*,<sup>†,§</sup> 

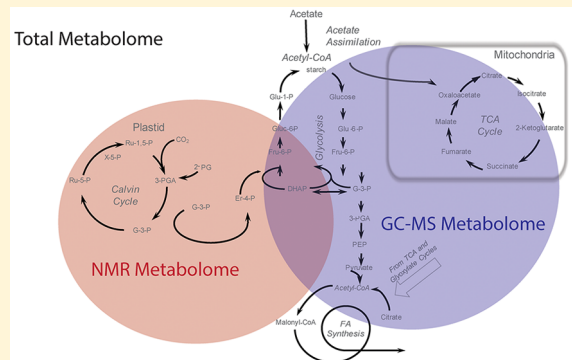
<sup>†</sup>Department of Chemistry, University of Nebraska, Lincoln, Nebraska 68588-0304, United States

<sup>‡</sup>Department of Biochemistry, University of Nebraska, Lincoln, Nebraska 68588-0664, United States

<sup>§</sup>Nebraska Center for Integrated Biomolecular Communication, Lincoln, Nebraska 68588-0304, United States

## Supporting Information

**ABSTRACT:** Despite inherent complementarity, nuclear magnetic resonance spectroscopy (NMR) and mass spectrometry (MS) are routinely separately employed to characterize metabolomics samples. More troubling is the erroneous view that metabolomics is better served by exclusively utilizing MS. Instead, we demonstrate the importance of combining NMR and MS for metabolomics by using small chemical compound treatments of *Chlamydomonas reinhardtii* as an illustrative example. A total of 102 metabolites were detected (82 by gas chromatography–MS, 20 by NMR, and 22 by both techniques). Out of these, 47 metabolites of interest were identified: 14 metabolites were uniquely identified by NMR, and 16 metabolites were uniquely identified by GC–MS. A total of 17 metabolites were identified by both NMR and GC–MS. In general, metabolites identified by both techniques exhibited similar changes upon compound treatment. In effect, NMR identified key metabolites that were missed by MS and enhanced the overall coverage of the oxidative pentose phosphate pathway, Calvin cycle, tricarboxylic acid cycle, and amino acid biosynthetic pathways that informed on pathway activity in central carbon metabolism, leading to fatty-acid and complex-lipid synthesis. Our study emphasizes a prime advantage of combining multiple analytical techniques: the improved detection and annotation of metabolites.



Metabolomics is experiencing exponential growth<sup>1</sup> and has made substantial contributions to various research areas, such as nutrition, plant physiology, cellular metabolism, disease diagnosis and biomarker detection, and drug discovery and development.<sup>2–45,6</sup> To date, metabolomics has primarily relied on the separate application of mass spectrometry (MS) or nuclear magnetic resonance spectroscopy (NMR), but there are also notable examples of the application of surface enhanced Raman spectroscopy and Fourier transform infrared spectroscopy (FTIR).<sup>7</sup> Nevertheless, the vast majority of recently published metabolomics studies are only making use of GC–MS or liquid chromatography (LC)–MS despite prior contributions from NMR and other analytical techniques.<sup>8</sup> In 2017, only 5% of metabolomics manuscripts published in PubMed described any form of a combined NMR and GC–MS approach to metabolomics (Figure 1). This may be explained, in part, by an erroneous belief that mass spectrometry is the optimal analytical technique for metabolomics. Unfortunately, this false perspective has begun to negatively impact the field and will likely limit the coverage of the metabolome, potentially diminish the quality of research, and hamper progress. Instead, metabolomics should seek to maximize (not limit) the number of analytical techniques used to characterize the entirety of the metabolome. Moreover, the confidence and accuracy of metabolite identification and

quantification is improved by the application of multiple analytical techniques. Thus, the goal of the field should be to accurately address scientific questions by striving for the broadest coverage of the metabolome, not by focusing on the type of instrumentation used.

NMR and MS are inherently complementary due to their distinct strengths and weaknesses. This, in turn, leads to different sets of metabolites that are uniquely detected by NMR and MS. Accordingly, combining both NMR and MS will result in a greater coverage of the metabolome. Simplistically, NMR detects the most-abundant metabolites, and MS detects the metabolites that are readily ionizable. This arises from fundamental differences between NMR and MS. For example, NMR requires minimal sample handling, but chromatography is a necessary component of MS metabolomics because of the relatively narrow molecular-weight distribution of the metabolome.<sup>9</sup> Chromatography methods are plagued by non-uniform metabolite derivatization, incomplete column recovery, decomposition during derivatization, ion-suppression due to the coeluent matrix, and misaligned retention times, to name a few reasons.<sup>10–14</sup> Similarly, small molecules exhibit variable thermal stability that

Received: July 24, 2018

Published: October 10, 2018

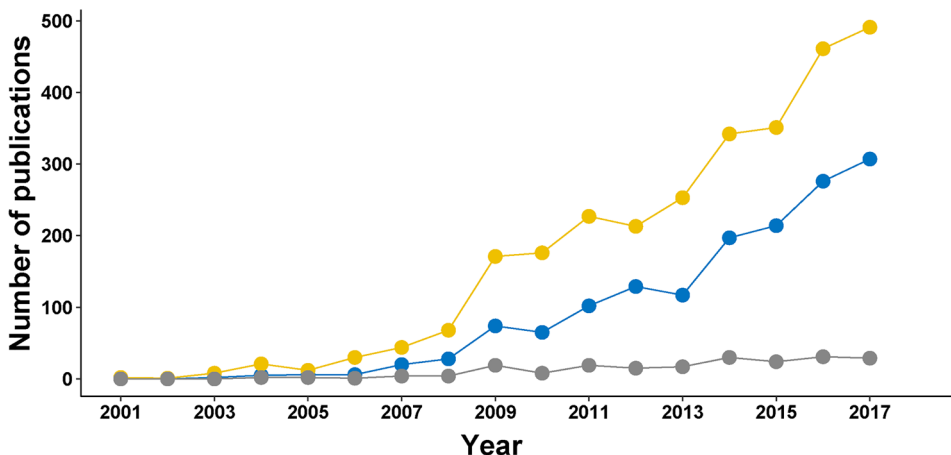


**Figure 1.** Summary of metabolomics publications in PubMed that refer only to NMR (yellow), only to GC-MS (blue), or to both GC-MS and NMR (gray).

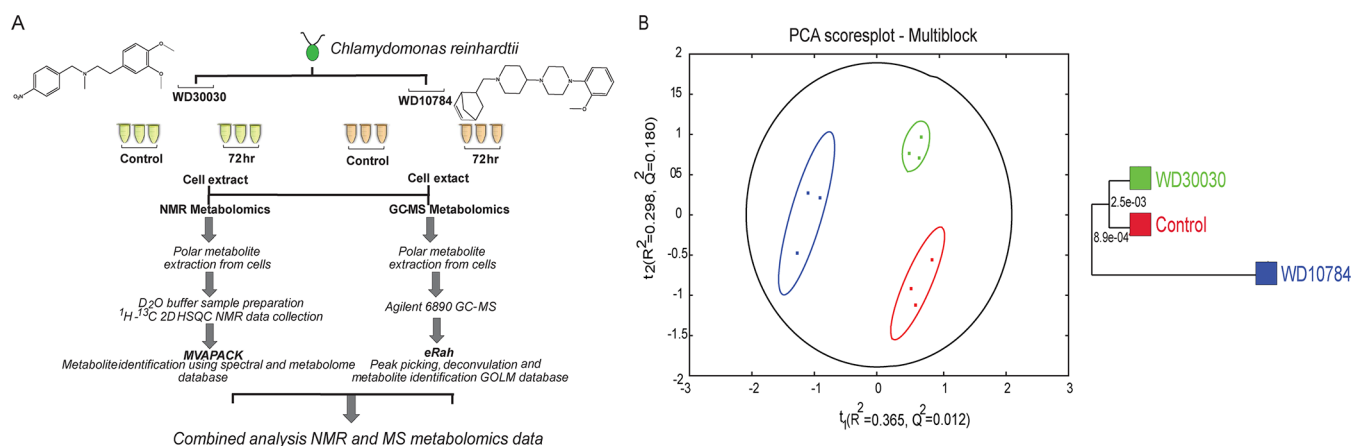


**Figure 2.** (A) Workflow schematic showing the key steps in the combined NMR and GC-MS analysis of the *C. reinhardtii* metabolome. Three biological replicates were prepared for each group consisting of the untreated controls, WD30030-treated cells, and WD10784-treated cells. A GC-MS spectrum and a 2D  $^1\text{H}$ - $^{13}\text{C}$  HSQC NMR spectrum were collected for each biological replicate. (B) Multiblock PCA scores plot generated from the combined GC-MS and 2D  $^1\text{H}$ - $^{13}\text{C}$  HSQC NMR data sets illustrating a distinct clustering for untreated controls (red squares) and the WD30030- (green squares) and WD10784- (blue squares) treated cells. A total of three biological replicates are displayed per group, and each data point represents the combined GC-MS and 2D  $^1\text{H}$ - $^{13}\text{C}$  HSQC NMR data sets plotted in the PC space. The ellipses represent a 95% confidence limit of the normal distribution of each cluster. The associated dendrogram was derived from the PCA scores plot, and each node is annotated with a Mahalanobis distance-based  $p$  value. The separation between untreated controls and WD30030 ( $p$  value of  $2.5 \times 10^{-3}$ ) and WD10784 ( $p$  value of  $8.9 \times 10^{-4}$ ), respectively, is considered statistically significant ( $p < 0.05$ ). The color scheme for the dendrogram is the same as the scores plot.

73 may lead to the loss of metabolites and the erroneous  
74 accumulation of degradation products at temperatures  
75 routinely used for gas chromatography (GC).<sup>15</sup> Conversely,  
76 NMR lacks the sensitivity to detect metabolites in the  
77 submicromolar range ( $\geq 1 \mu\text{M}$ ) and has limited spectral  
78 resolution that often results in peak overlap.<sup>16</sup> MS also has a  
79 higher resolution ( $\sim 10^3$  to  $10^4$ ) and dynamic range ( $\sim 10^3$  to  
80  $10^4$ ) relative to NMR.

81 Ambiguous peak assignments are a common problem  
82 encountered by both NMR and MS. This issue is attributed  
83 to limitations in the availability of reference spectra, insufficient  
84 software and databases, and our incomplete knowledge of the  
85 metabolome. It is believed that nearly all metabolomics  
86 investigations have at least one misidentified or unidentified  
87 metabolite.<sup>17</sup> Natural product chemistry has routinely  
88 employed protocols involving both NMR and MS data to  
89 identify novel compounds, but the application of this  
90 combinatorial approach has seen limited usage in metabo-  
91 lomics.<sup>18</sup> Nevertheless, a few methods have recently been

described that combine NMR and MS to assign metabolites  
92 and identify unknowns.<sup>19-21</sup> Notably, the community has  
93 recognized that metabolomics needs to continue to move in  
94 this direction.<sup>8,21-26</sup> There have also been a few recent  
95 examples that highlight the utility and complementarity of  
96 combining 1D  $^1\text{H}$  NMR with direct injection or LC- and  
97 GC-MS experiments for metabolomics.<sup>27,28</sup> Most of these  
98 examples are methodology-driven; are focused on improving  
99 statistical tools and modeling; or performed parallel, but  
100 separate, sample analysis.<sup>29-31</sup> In this regards, NMR is  
101 routinely only used as a supplement to MS or in a secondary  
102 confirmatory role. Accordingly, the full impact of using NMR  
103 to characterize a metabolomics sample is missed.  
104

105 Current estimates suggest the size of the human  
metabolome is approximately 150 000 metabolites, but only  
106 those upward of a few hundred metabolites are typically  
107 identified in a given metabolomics study.<sup>32</sup> Combining MS  
108 with NMR and other analytical techniques is necessary to  
109 move beyond this self-imposed limit.  
110

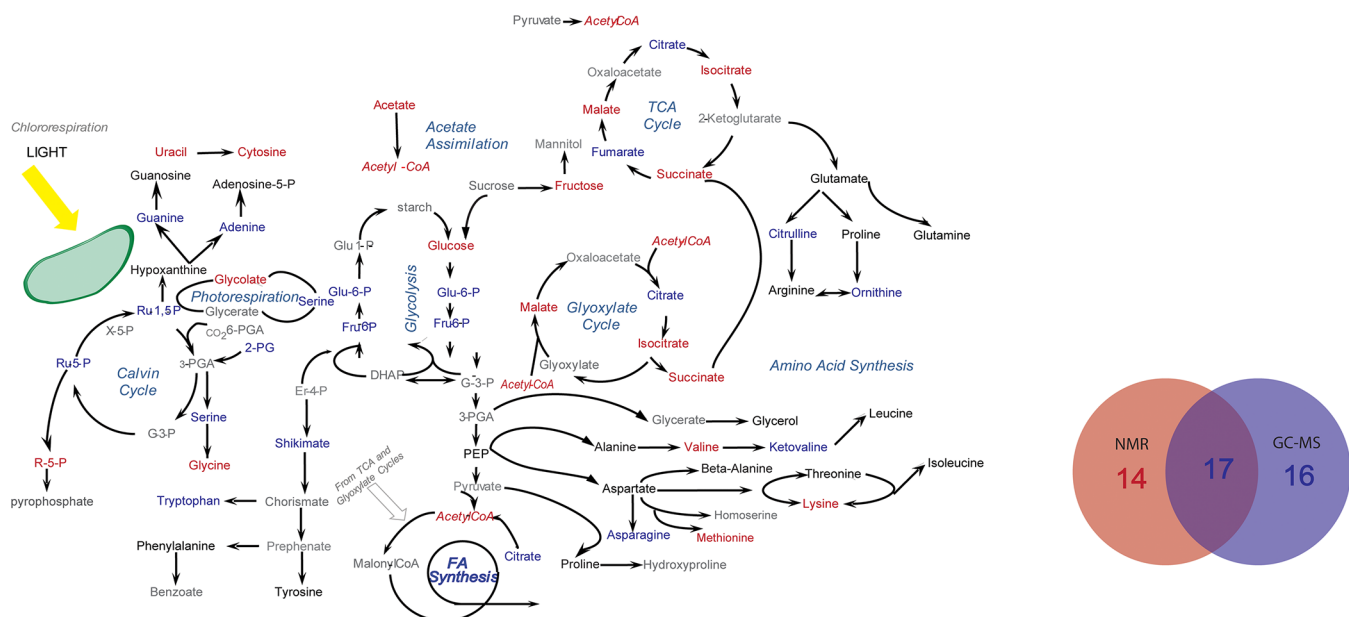


**Figure 3.** Metabolic pathway summarizing the coverage of the *C. reinhardtii* metabolome (metabolites of interest) from the combined application of NMR and GC-MS. Metabolites that were only identified by NMR are colored blue. Metabolites that were only identified by GC-MS are colored red. Metabolites identified by both methods are colored black, and metabolites that are not identified are colored gray. The embedded Venn diagram identifies the total number of metabolites of interest within these metabolic pathways that were identified either by NMR, by GC-MS, or by both techniques.

111 To address this need, a global metabolomics study was  
 112 performed in a platform-unbiased fashion to highlight the  
 113 intrinsic benefits of combining NMR and MS. In this regard,  
 114 NMR and MS data were collected on a similar set of samples  
 115 without complicating existing workflows or requiring major  
 116 protocol modifications. Accordingly, there were no serious  
 117 experimental barriers encountered that would prevent the  
 118 metabolomics community from adapting a combined NMR  
 119 and MS approach as a standard for the field. As an illustrated  
 120 example, the metabolome of *Chlamydomonas reinhardtii* grown  
 121 in tris-acetate phosphate (TAP) media ( $^{13}\text{C}_2$ -acetate for  
 122 NMR) was characterized by NMR and GC-MS. The cells  
 123 were also treated with two lipid accumulation modulators  
 124 (WD30030 and WD10784) as described by Wase et al.<sup>33</sup> The  
 125 aqueous-extracted metabolomes from treated and untreated  
 126 cells were then compared to identify metabolic variations due  
 127 to the compound treatments. The eRah package was used to  
 128 perform peak picking, retention-time alignment, and metabo-  
 129 lite library search for the GC-MS data set.<sup>33,34</sup> Similarly,  
 130 NMRpipe<sup>35</sup> and NMRviewJ<sup>36</sup> were used for processing and  
 131 peak picking the NMR data set and metabolite assignments  
 132 were performed using spectral databases.<sup>37</sup> A schematic  
 133 overview of the workflow is shown in Figure 2A. Details of  
 134 data handling, processing and analyses are available as  
 135 Supporting Information.

136 The complete 2D  $^1\text{H}$ - $^{13}\text{C}$  HSQC NMR spectra obtained  
 137 from *C. reinhardtii* metabolome extracts were used for  
 138 unsupervised multivariate analyses to generate a principal  
 139 component analyses (PCA) scores plot with an associated  
 140 dendrogram (Figure S-1A). Statistical models were generated  
 141 after the data was processed as a matrix to be standard normal  
 142 variate (SNV) normalized and unit variance scaled. The  
 143 WD30030- and WD10784-treated cells formed distinct  
 144 clusters separate from the untreated control. The dendrogram  
 145 generated from the Mahalanobis distances between each point  
 146 in the PCA scores plot and the resulting  $p$  value between each

node indicates a statistically significant ( $p < 0.05$ ) separation 147 between each group. Similarly, metabolite assignments from 148 the GC-MS spectral data set were obtained from the eRah 149 package and identified using the GOLM database.<sup>38</sup> The 150 assigned metabolite peak areas were then imported as a matrix 151 into MVAPACK to obtain a comparable PCA scores plot and 152 dendrogram as described above (Figure S-1B).<sup>39</sup> A similar 153 statistically significant group separation between the 154 WD30030- and WD10784-treated cells and the untreated 155 controls was obtained. Importantly, the NMR and GC-MS 156 data sets were successfully combined to generate a comparable 157 multiblock (MB)-principal component analysis (PCA) model 158 with a corresponding dendrogram (Figure 2B).<sup>30</sup> The MB- 159 PCA model provides a single statistical model for both data 160 sets. In this manner, key metabolite differences between the 161 treated and untreated controls can be identified irrespective of 162 the analytical method. 163

Overall, 82 compounds were identified by GC-MS alone 164 and 20 by NMR alone, and 22 were common to both methods 165 (Tables S-1–S-3). Of these 102 detected metabolites, a total of 166 47 metabolites of interest were perturbed upon compound- 167 induced changes in the *C. reinhardtii* metabolome was obtained 169 by combining the metabolite assignments from the NMR and 170 GC-MS data sets. Specifically, 14 unique metabolites were 171 identified from the NMR analysis of  $^{13}\text{C}_2$ -acetate labeled *C. 172 reinhardtii* cells that were significantly perturbed upon 173 treatment with either WD30030 or WD10784. Metabolites 174 were assigned using the Biological Magnetic Resonance Bank 175 (BMRB) metabolomics database.<sup>40</sup> Similarly, 16 unique 176 metabolites were identified from the GC-MS spectra using 177 the GOLM database. Furthermore, an additional 17 metabo- 178 lites were identified by both NMR and GC-MS. In total, the 179 metabolites comprise the following metabolic pathways: the 180 oxidative pentose phosphate pathway, the Calvin cycle, the 181 tricarboxylic acid cycle, and the amino acid biosynthetic 182

183 pathways. A summary of the *C. reinhardtii* metabolic changes  
184 of interest resulting from treatment with WD30030 and  
185 WD10784 is shown in [Figure 3](#).

186 NMR and GC-MS identified nine glycolytic intermediates  
187 in which fructose, glycerol, and pyruvate were uniquely  
188 identified by NMR, and fructose-6-phosphate was unique to  
189 GC-MS. All 20 amino acids were detected from the combined  
190 data sets, but asparagine, cysteine, histidine, serine, and  
191 tryptophan were only observed with GC-MS. Consequently,  
192 glycine, lysine, methionine, and valine were unique to NMR.  
193 Tricarboxylic acid cycle and Calvin cycle metabolites exhibited  
194 the most variation. Acetate, isocitrate, ketoglutarate, malate,  
195 and succinate were identified by NMR, but fumarate was  
196 limited to GC-MS. Ribulose and its phosphate derivatives  
197 were exclusively assigned through GC-MS. Nucleotide and  
198 nucleoside analogs were the metabolite group consistently  
199 observed by both techniques. A total of 7 out of the 10  
200 metabolites (2-deoxy adenosine, adenosine, guanosine, hypo-  
201 xanthine, inosine, thymine, and xanthosine) were observed by  
202 both NMR and GC-MS. Cytosine and uridine were uniquely  
203 identified by NMR, whereas uracil was only observed by GC-  
204 MS. A complete list of metabolites identified by NMR and GC  
205 are provided in [Tables S-1–S-4](#).

206 The complete set of 22 metabolites identified by both NMR  
207 and GC-MS, including the 17 metabolites of interest depicted  
208 in [Figure 3](#), were further evaluated for overall consistency  
209 between the two methods. A correlation between the 22  
210 common metabolites was evaluated using Pearson correlation  
211 within the R environment (<http://www.r-project.org>), and the  
212 resulting comparison is plotted in [Figure 4](#). While there is  
213 significant scatter, the overall trend is quite similar. It is  
214 important to note that only relative changes in metabolite  
215 concentrations were compared. Furthermore, the GC-MS  
216 metabolomics analysis was untargeted and lacked any  
217 metabolite-specific calibration. Conversely, the absolute  
218 quantitation of metabolite concentration changes is an

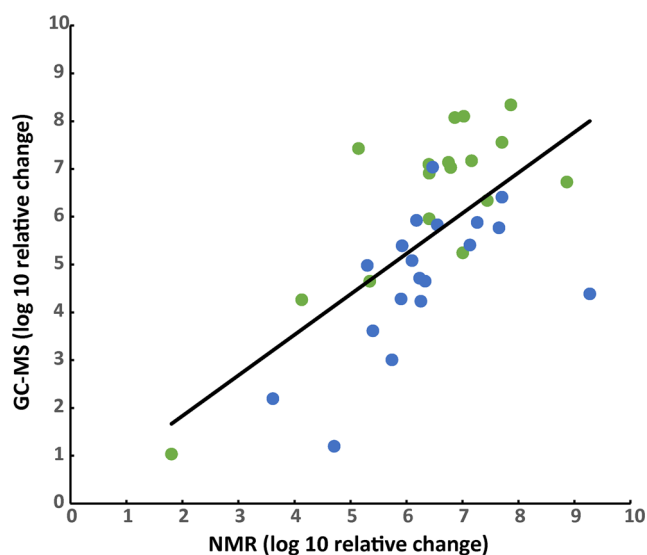


**Figure 4.** Comparison of the 22 relative metabolite concentration changes detected by NMR and GC-MS. Metabolite changes resulting from treatment with WD30030 and WD10784 are colored green or blue, respectively. The regression line fitted to the data exhibited a correlation coefficient of  $R^2$  0.55 and a confidence interval with a  $p$  value of  $<0.001$ .

219 inherent strength of NMR. However, NMR was only used to 219  
220 monitor the relative changes in metabolites derived from  $^{13}\text{C}_2$ - 220  
acetate, whereas GC-MS captured total metabolite changes. 221  
Differences in the number of sample processing steps may also 222  
impart unintended variations. Metabolite derivatization has 223  
been identified as a major source of sample variation.<sup>10,12,14</sup> 224  
Similarly, variable metabolite stability during GC-MS data 225  
acquisition is another potential source of error.<sup>15</sup> Finally, a 226  
limited number of biological replicates will also contribute to a 227  
larger variance. We want to emphasize that, given these 228  
unavoidable discrepancies and the limited number of sample 229  
replicates, the observed correlation between the relative 230  
changes in metabolite concentration is quite notable. 231  
Importantly, the overall trend (or direction) in metabolite 232  
concentration change is preserved for the majority of 233  
metabolites despite the scatter in the magnitude of these 234  
changes. Furthermore, a simple comparison of metabolite 235  
trends is probably the limit of the data given the distinct and 236  
numerous sources of variance. 237

238 A pair-wise comparison between the 22 individual 238  
metabolites identified by both NMR and GC-MS are plotted 239  
as line curves in [Figure S2](#). Again, an acceptable level of 240  
consistency is achieved in the pair-wise comparisons. A general 241  
agreement was also observed in the relative changes between 242  
both compound treatments. Any observed discrepancies 243  
between metabolite trends may be explained by the fact that 244  
GC-MS is capturing the total metabolite change, while NMR 245  
is only capturing the changes in metabolites derived from  $^{13}\text{C}_2$ - 246  
acetate. In this regard, both measurements are likely correct 247  
but are simply observing different aspects of the metabolome. 248  
Again, this highlights the inherent strength of combining both 249  
NMR and MS. Conversely, if GC-MS observes a significantly 250  
lower metabolite concentration relative to NMR, this is a likely 251  
an error in the GC-MS data due to a limited thermal stability 252  
of the metabolite, variations in derivatization efficiency, and 253  
the multiplet phenomena.<sup>12–15</sup> Additionally, given the fact 254  
that NMR routinely provides highly accurate sample 255  
quantitation relative to MS, NMR is likely to provide the 256  
correct metabolite change when the methods disagree ([Figure 257](#)  
S3).<sup>41</sup> 258

259 Extensive (nearly complete) coverage of key metabolic 259  
pathways associated with lipid accumulation was only achieved 260  
by combining NMR and GC-MS data. In effect, the NMR 261  
data filled-in the metabolites that were missed by GC-MS. 262  
Importantly, the broader coverage of the *C. reinhardtii* 263  
metabolome was able to provide a comprehensive view of 264  
the algae's response to a compound treatment. This level of 265  
detail is essential to further our understanding of the 266  
mechanism of action of drug leads, of drug resistance, and of 267  
disease development and progression, among numerous other 268  
potential utilities. Achieving this level of coverage of the 269  
metabolome requires employing multiple analytical techniques. 270  
This viewpoint is consistent with some prior observa- 271  
tions.<sup>8,21–26</sup> For example, Chen et al. noted an improvement 272  
in biomarker identification by combining 1D  $^1\text{H}$  NMR and 273  
GC-MS for the analysis of urine from patients with bipolar 274  
disorder.<sup>42</sup> Another recent example highlighted the use of 1D 275  
 $^1\text{H}$  NMR and GC-MS for the analysis of bronchial-wash fluid 276  
to investigate responsiveness to air pollution.<sup>43</sup> Barding et al. 277  
have highlighted similar improvements in coverage of the 278  
metabolome in molecular response of rice to stress.<sup>44</sup> These 279  
studies were able to combine multiple data sets to obtain a 280  
robust set of biomarkers, which further emphasizes the benefit 281

282 of combining multiple analytical platforms for metabolomics.  
 283 These are other recent examples in which both NMR and  
 284 GC-MS metabolomics data sets have been integrated for  
 285 applications in biomarker identification, food chemistry, and  
 286 plant physiology.<sup>45-48</sup>

287 To date, the majority of metabolomics studies have been  
 288 self-limited to a single analytical platform (Figure 1). This is  
 289 despite the fact that NMR and MS (and other analytical  
 290 techniques) are highly complementary. Furthermore, existing  
 291 workflows (Figure 2A) can easily accommodate the inclusion  
 292 of both techniques. Consequently, there is little to no barrier to  
 293 the broad adoption by the scientific community of a  
 294 multianalytical approach to metabolomics. Importantly, and  
 295 as clearly demonstrated herein, combining NMR and MS  
 296 improves the coverage of the metabolome, increases the  
 297 accuracy of metabolite assignments,<sup>19-21</sup> and provides  
 298 redundant validation of metabolite changes. In fact, our results  
 299 demonstrate a limited overlap in the metabolites identified by  
 300 both NMR and GC-MS. However, most metabolites in  
 301 common did exhibit consistent trends in relative concentration  
 302 changes, showcasing the robustness of the combined approach.  
 303 Our results provide clear evidence that both NMR and MS are  
 304 equally valuable and necessary for metabolomics studies and  
 305 that combining multiple analytical sources is essential to the  
 306 future of metabolomics.

## 307 ■ ASSOCIATED CONTENT

### 308 ■ Supporting Information

309 The Supporting Information is available free of charge on the  
 310 ACS Publications website at DOI: 10.1021/acs.jproteome.8b00567.

312 Additional experimental methods; figures showing PCA  
 313 scores plots, individual line plots, and a comparison of  
 314 metabolite changes; tables showing lists of metabolites  
 315 uniquely identified with analysis methods and a  
 316 comparison of metabolites of interest (PDF)

## 317 ■ AUTHOR INFORMATION

### 318 Corresponding Author

319 \*E-mail: rpowers3@unl.edu; phone: (402) 472-3039; fax:  
 320 (402) 472-9402.

### 321 ORCID

322 Robert Powers: 0000-0001-9948-6837

### 323 Author Contributions

324 F.B. and N.W. performed the experiments; R.P. and C.D.  
 325 designed the experiments; F.B., N.W., C.D., and R.P. analyzed  
 326 the data and wrote the manuscript.

### 327 Notes

328 The authors declare no competing financial interest.

## 329 ■ ACKNOWLEDGMENTS

330 We thank Dr. Martha Morton, the Director of the Research  
 331 Instrumentation Facility in the Department of Chemistry at  
 332 the University of Nebraska-Lincoln, for her assistance with the  
 333 NMR experiments. This material is based on work supported  
 334 by the National Science Foundation under grant no. 1660921.  
 335 This work was supported in part by funding from the Redox  
 336 Biology Center (P30 GM103335, NIGMS) and the Nebraska  
 337 Center for Integrated Biomolecular Communication (P20  
 338 GM113126, NIGMS). The research was performed in facilities

339 renovated with support from the National Institutes of Health 339  
 (RR015468-01). Any opinions, findings, and conclusions or 340  
 recommendations expressed in this material are those of the 341  
 author(s) and do not necessarily reflect the views of the 342  
 National Science Foundation. 343

## ■ REFERENCES

- (1) Powers, R. The Current State of Drug Discovery and a Potential Role for NMR Metabolomics. *J. Med. Chem.* **2014**, *57* (14), 5860–5870.
- (2) Bradley, S. A.; Ouyang, A.; Purdie, J.; Smitka, T. A.; Wang, T.; Kaerner, A. Fermentanomics: Monitoring Mammalian Cell Cultures with NMR Spectroscopy. *J. Am. Chem. Soc.* **2010**, *132* (28), 9531–9533.
- (3) von Reuss, S. H.; Bose, N.; Srinivasan, J.; Yim, J. J.; Judkins, J. C.; Sternberg, P. W.; Schroeder, F. C. Comparative Metabolomics Reveals Biogenesis of Ascarosides, a Modular Library of Small Molecule Signals in *C. elegans*. *J. Am. Chem. Soc.* **2012**, *134* (3), 1817–1824.
- (4) Vizcaino, M. I.; Engel, P.; Trautman, E.; Crawford, J. M. Comparative Metabolomics and Structural Characterizations Illuminate Colibactin Pathway-Dependent Small Molecules. *J. Am. Chem. Soc.* **2014**, *136* (26), 9244–9247.
- (5) Kalisiak, J.; Trauger, S. A.; Kalisiak, E.; Morita, H.; Fokin, V. V.; Adams, M. W. W.; Sharpless, K. B.; Siuzdak, G. Identification of a New Endogenous Metabolite and the Characterization of Its Protein Interactions through an Immobilization Approach. *J. Am. Chem. Soc.* **2009**, *131* (1), 378–386.
- (6) Espaillat, A.; Forsmo, O.; El Biari, K.; Björk, R.; Lemaitre, B.; Trygg, J.; Cañada, F. J.; de Pedro, M. A.; Cava, F. Chemometric Analysis of Bacterial Peptidoglycan Reveals Atypical Modifications That Empower the Cell Wall against Predatory Enzymes and Fly Innate Immunity. *J. Am. Chem. Soc.* **2016**, *138* (29), 9193–9204.
- (7) Ali, M. R. K.; Wu, Y.; Han, T.; Zang, X.; Xiao, H.; Tang, Y.; Wu, R.; Fernández, F. M.; El-Sayed, M. A. Simultaneous Time-Dependent Surface-Enhanced Raman Spectroscopy, Metabolomics, and Proteomics Reveal Cancer Cell Death Mechanisms Associated with Gold Nanorod Photothermal Therapy. *J. Am. Chem. Soc.* **2016**, *138* (47), 15434–15442.
- (8) Marshall, D. D.; Powers, R. Beyond the paradigm: Combining mass spectrometry and nuclear magnetic resonance for metabolomics. *Prog. Nucl. Magn. Reson. Spectrosc.* **2017**, *100*, 1–16.
- (9) Kell, D. B. Metabolomics and systems biology: making sense of the soup. *Curr. Opin. Microbiol.* **2004**, *7* (3), 296–307.
- (10) Xu, F.; Zou, L.; Ong, C. N. Multiorigination of chromatographic peaks in derivatized GC/MS metabolomics: A confounder that influences metabolic pathway interpretation. *J. Proteome Res.* **2009**, *8* (12), 5657–5665.
- (11) Kanani, H.; Chrysanthopoulos, P. K.; Klapa, M. I. Standardizing GC-MS metabolomics. *J. Chromatogr. B: Anal. Technol. Biomed. Life Sci.* **2008**, *871* (2), 191–201.
- (12) Halket, J. M.; Waterman, D.; Przyborowska, A. M.; Patel, R. K. P.; Fraser, P. D.; Bramley, P. M. Chemical derivatization and mass spectral libraries in metabolic profiling by GC/MS and LC/MS/MS. *J. Exp. Bot.* **2005**, *56* (410), 219–243.
- (13) Xu, F.; Zou, L.; Ong, C. N.; Zou, L.; Ong, C. N. Experiment originated variations, and multi-peak and multi-origination phenomena in derivatization-based GC-MS metabolomics. *TrAC, Trends Anal. Chem.* **2010**, *29* (3), 269–280.
- (14) Moros, G.; Chatzioannou, A. C.; Gika, H. G.; Raikos, N.; Theodoridis, G. Investigation of the derivatization conditions for GC-MS metabolomics of biological samples. *Bioanalysis* **2017**, *9* (1), 53–65.
- (15) Fang, M.; Ivanisevic, J.; Benton, H. P.; Johnson, C. H.; Patti, G. J.; Hoang, L. T.; Uritboonthai, W.; Kurczy, M. E.; Siuzdak, G. Thermal Degradation of Small Molecules: A Global Metabolomic Investigation. *Anal. Chem.* **2015**, *87* (21), 10935–10941.

405 (16) Pan, Z.; Raftery, D. Comparing and combining NMR  
406 spectroscopy and mass spectrometry in metabolomics. *Anal. Bioanal.*  
407 *Chem.* **2007**, *387* (2), 525–527.

408 (17) Bird, S. S.; Sheldon, D. P.; Gathungu, R. M.; Vouros, P.; Kautz,  
409 R.; Matson, W. R.; Kristal, B. S. Structural characterization of plasma  
410 metabolites detected via LC-electrochemical coulometric array using  
411 LC-UV fractionation, MS, and NMR. *Anal. Chem.* **2012**, *84* (22),  
412 9889–9898.

413 (18) Forseth, R. R.; Fox, E. M.; Chung, D.; Howlett, B. J.; Keller, N.  
414 P.; Schroeder, F. C. Identification of Cryptic Products of the  
415 Gliotoxin Gene Cluster Using NMR-Based Comparative Metabolo-  
416 mics and a Model for Gliotoxin Biosynthesis. *J. Am. Chem. Soc.* **2011**,  
417 *133* (25), 9678–9681.

418 (19) Wang, C.; He, L.; Li, D.-W.; Bruschweiler-Li, L.; Marshall, A.  
419 G.; Bruschweiler, R. Accurate Identification of Unknown and Known  
420 Metabolic Mixture Components by Combining 3D NMR with  
421 Fourier Transform Ion Cyclotron Resonance Tandem Mass  
422 Spectrometry. *J. Proteome Res.* **2017**, *16* (10), 3774–3786.

423 (20) Bingol, K.; Bruschweiler, R. Knowns and unknowns in  
424 metabolomics identified by multidimensional NMR and hybrid MS/  
425 NMR methods. *Curr. Opin. Biotechnol.* **2017**, *43*, 17–24.

426 (21) Bingol, K.; Brueschweiler, R. Two elephants in the room: new  
427 hybrid nuclear magnetic resonance and mass spectrometry approaches  
428 for metabolomics. *Curr. Opin. Clin. Nutr. Metab. Care* **2015**, *18* (5),  
429 471–477.

430 (22) Stryeck, S.; Madl, T.; Birner-Gruenberger, R. Integrative  
431 metabolomics as emerging tool to study autophagy regulation. *Microb.*  
432 *Cell* **2017**, *4* (8), 240–258.

433 (23) Bruntz, R. C.; Lane, A. N.; Higashi, R. M.; Fan, T. W. M.  
434 Exploring cancer metabolism using stable isotope-resolved metabo-  
435 lomics (SIRM). *J. Biol. Chem.* **2017**, *292* (28), 11601–11609.

436 (24) Gonzalez-Dominguez, A.; Duran-Guerrero, E.; Fernandez-  
437 Recamales, A.; Lechuga-Sancho, A. M.; Sayago, A.; Schwarz, M.;  
438 Segundo, C.; Gonzalez-Dominguez, R. An Overview on the  
439 Importance of Combining Complementary Analytical Platforms in  
440 Metabolomic Research. *Curr. Top. Med. Chem. (Sharjah, United Arab*  
441 *Emirates)* **2018**, *17* (30), 3289–3295.

442 (25) Bingol, K. Recent Advances in Targeted and Untargeted  
443 Metabolomics by NMR and MS/NMR Methods. *High Throughput*  
444 **2018**, *7* (2), 9.

445 (26) Pan, Z.; Raftery, D. Comparing and combining NMR  
446 spectroscopy and mass spectrometry in metabolomics. *Anal. Bioanal.*  
447 *Chem.* **2007**, *387* (2), 525–527.

448 (27) Bingol, K.; Brüschweiler, R. NMR/MS translator for the  
449 enhanced simultaneous analysis of metabolomics mixtures by NMR  
450 spectroscopy and mass spectrometry: Application to human urine. *J.*  
451 *Proteome Res.* **2015**, *14* (6), 2642–2648.

452 (28) Bingol, K.; Bruschweiler-Li, L.; Yu, C.; Somogyi, A.; Zhang, F.;  
453 Brüschweiler, R. Metabolomics beyond Spectroscopic Databases: A  
454 Combined MS/NMR Strategy for the Rapid Identification of New  
455 Metabolites in Complex Mixtures. *Anal. Chem.* **2015**, *87* (7), 3864–  
456 3870.

457 (29) Baker, J. M.; Ward, J. L.; Beale, M. H. Combined NMR and  
458 Flow Injection ESI-MS for brassicaceae metabolomics. *Methods Mol.*  
459 *Biol.* **2011**, *860*, 177–191.

460 (30) Marshall, D. D.; Lei, S.; Worley, B.; Huang, Y.; Garcia-Garcia,  
461 A.; Franco, R.; Dodds, E. D.; Powers, R. Combining DI-ESI-MS and  
462 NMR datasets for metabolic profiling. *Metabolomics* **2015**, *11* (2),  
463 391–402.

464 (31) Farag, M. A.; Porzel, A.; Schmidt, J.; Wessjohann, L. A.  
465 Metabolite profiling and fingerprinting of commercial cultivars of  
466 *Humulus lupulus* L. (hop): a comparison of MS and NMR methods  
467 in metabolomics. *Metabolomics* **2012**, *8* (3), 492–507.

468 (32) Markley, J. L.; Brüschweiler, R.; Edison, A. S.; Eghbalnia, H. R.;  
469 Powers, R.; Raftery, D.; Wishart, D. S. The future of NMR-based  
470 metabolomics. *Curr. Opin. Biotechnol.* **2017**, *43*, 34–40.

471 (33) Wase, N.; Tu, B.; Allen, J. W.; Black, P. N.; DiRusso, C. C.  
472 Identification and Metabolite Profiling of Chemical Activators of  
Lipid Accumulation in Green Algae. *Plant Physiol.* **2017**, *174* (4), 473  
2146. 474

473 (34) Domingo-Almenara, X.; Brezmes, J.; Vinaixa, M.; Samino, S.;  
474 Ramirez, N.; Ramon-Krauel, M.; Lerin, C.; Diaz, M.; Ibanez, L.;  
475 Correig, X.; Perera-Lluna, A.; Yanes, O. eRah: A Computational Tool  
476 Integrating Spectral Deconvolution and Alignment with Quantifica-  
477 tion and Identification of Metabolites in GC/MS-Based Metabolo-  
478 mics. *Anal. Chem.* **2016**, *88* (19), 9821–9829. 479

479 (35) Delaglio, F.; Grzesiek, S.; Vuister, G. W.; Zhu, G.; Pfeifer, J.;  
480 Bax, A. NMRPipe: a multidimensional spectral processing system  
481 based on UNIX pipes. *J. Biomol. NMR* **1995**, *6* (3), 277–93. 482

482 (36) Johnson, B. A. From Raw Data to Protein Backbone Chemical  
483 Shifts Using NMRFX Processing and NMRViewJ Analysis. *Methods*  
484 *Mol. Biol.* **2018**, *1688*, 257–310. 485

485 (37) Ulrich, E. L.; Akutsu, H.; Doreleijers, J. F.; Harano, Y.;  
486 Ioannidis, Y. E.; Lin, J.; Livny, M.; Mading, S.; Maziuk, D.; Miller, Z.;  
487 Nakatani, E.; Schulte, C. F.; Tolmie, D. E.; Kent Wenger, R.; Yao, H.;  
488 Markley, J. L. BioMagResBank. *Nucleic Acids Res.* **2007**, *36*, D402. 490

489 (38) Kopka, J.; Schauer, N.; Krueger, S.; Birkemeyer, C.; Usadel, B.;  
490 Bergmüller, E.; Dörmann, P.; Weckwerth, W.; Gibon, Y.; Stitt, M.;  
491 Willmitzer, L.; Fernie, A. R.; Steinhauser, D. GMD@CSB.DB: the  
492 Golm Metabolome Database. *Bioinformatics* **2005**, *21* (8), 1635–  
493 1638. 494

494 (39) Worley, B.; Powers, R. MVAPACK: A complete data handling  
495 package for NMR metabolomics. *ACS Chem. Biol.* **2014**, *9* (5), 1138–  
496 1144. 497

497 (40) Bingol, K.; Li, D.-W.; Bruschweiler-Li, L.; Cabrera, O. A.;  
498 Megraw, T.; Zhang, F.; Bruschweiler, R. Unified and Isomer-Specific  
499 NMR Metabolomics Database for the Accurate Analysis of 13C-1H  
500 HSQC Spectra. *ACS Chem. Biol.* **2015**, *10* (2), 452–459. 501

501 (41) Malz, F.; Jancke, H. Validation of quantitative NMR. *J. Pharm.*  
502 *Biomed. Anal.* **2005**, *38* (5), 813–823. 503

503 (42) Chen, J.; Liu, Z.; Fan, S.; Yang, D.; Zheng, P.; Shao, W.; Qi, Z.;  
504 Xu, X.; Li, Q.; Mu, J.; Yang, Y.; Xie, P. Combined Application of  
505 NMR- and GC-MS-Based Metabonomics Yields a Superior Urinary  
506 Biomarker Panel for Bipolar Disorder. *Sci. Rep.* **2015**, *4*, 5855. 507

507 (43) Surowiec, I.; Karimpour, M.; Gouveia-Figueira, S.; Wu, J.;  
508 Unosson, J.; Bosson, J. A.; Blomberg, A.; Pourazar, J.; Sandström, T.;  
509 Behndig, A. F.; Trygg, J.; Nording, M. L. Multi-platform  
510 metabolomics assays for human lung lavage fluids in an air pollution  
511 exposure study. *Anal. Bioanal. Chem.* **2016**, *408* (17), 4751–4764. 512

512 (44) Barding, G. A.; Béni, S.; Fukao, T.; Bailey-Serres, J.; Larive, C.;  
513 K. Comparison of GC-MS and NMR for Metabolite Profiling of Rice  
514 Subjected to Submergence Stress. *J. Proteome Res.* **2013**, *12* (2), 898–  
515 909. 516

516 (45) Griffith, C. M.; Morgan, M. A.; Dinges, M. M.; Mathon, C.;  
517 Larive, C. K. Metabolic Profiling of Chloroacetanilide Herbicides in  
518 Earthworm Coelomic Fluid Using <sup>1</sup>H NMR and GC-MS. *J. Proteome Res.*  
519 **2018**, *17* (8), 2611–2622. 520

520 (46) Kumar, A.; Maurya, A. K.; Chand, G.; Agnihotri, V. K. Comparative  
521 metabolic profiling of *Costus speciosus* leaves and  
522 rhizomes using NMR, GC-MS and UPLC/ESI-MS/MS. *Nat. Prod.*  
523 *Res.* **2018**, *32* (7), 826–833. 524

524 (47) Tomita, S.; Nakamura, T.; Okada, S. NMR- and GC/MS-based  
525 metabolomic characterization of sunki, an unsalted fermented pickle  
526 of turnip leaves. *Food Chem.* **2018**, *258*, 25–34. 527

527 (48) Trimigno, A.; Munger, L.; Picone, G.; Freiburghaus, C.;  
528 Pimentel, G.; Vionnet, N.; Pralong, F.; Capozzi, F.; Badertscher, R.;  
529 Vergeres, G. GC-MS Based Metabolomics and NMR Spectroscopy  
530 Investigation of Food Intake Biomarkers for Milk and Cheese in  
531 Serum of Healthy Humans. *Metabolites* **2018**, *8* (2), 26. 532